

Understanding Fluorescence Quenching in Polymers Obtained by RAFT

J. P. S. Farinha,^{*,†} Paula Relógio,^{†,‡} Marie-Thérèse Charreyre,[‡] T. J. V. Prazeres,^{†,‡} and J. M. G. Martinho[†]

Centro de Química-Física Molecular, Instituto Superior Técnico, 1049-001 Lisboa, Portugal, and
Unité Mixte CNRS-bioMérieux, Ecole Normale Supérieure de Lyon, 46 allée d'Italie,
69364 Lyon Cedex 07, France

Received February 19, 2007; Revised Manuscript Received April 20, 2007

ABSTRACT: Reversible addition–fragmentation chain transfer (RAFT) polymerization is a versatile process to obtain polymers with controlled architecture and molecular weight from a large variety of monomers. This appears to be a very attractive method for the synthesis of fluorescent polymers for different applications. However, fluorescent polymers obtained by RAFT are known to suffer strong fluorescence quenching. Here, we report the quenching of coumarin 343 (C343) fluorescence by four different chain transfer agents (CTA) used in RAFT polymerization: carboxymethyl dithiobenzoate (CMDDB), *tert*-butyl dithiobenzoate (*t*BDB), menthonyl dithiobenzoate (MDB), and bis(3-methylbutyl)-2-(thiobenzoylthio)succinate (MBTS). The quenching ability of these CTAs was compared with that of a macroCTA (poly(DcA)–MBTS) obtained from the RAFT polymerization of *N*-decylacrylamide (DcA) using MBTS as chain transfer agent. The results of stationary and time-resolved fluorescence measurements of C343 with the different CTA and macroCTA can be interpreted with a single kinetic model, which considers the reversible formation of a C343–CTA exciplex and both static and dynamic quenching of C343. The photophysical properties of *tert*-butyl mercaptan (*t*BM), resulting from the aminolysis of the *t*BDB dithioester, were also studied using the same experimental conditions, confirming that the thiol group does not quench the C343 fluorescence. This was further tested by converting poly(DcA)–MBTS to the corresponding thiol-ended chain, eliminating the fluorescence quenching of coumarin previously observed.

Introduction

In many applications of fluorescent polymers a large polydispersity in mass and number of dyes per chain disfavor their potential applications. To obtain polymer chains with well-defined architecture and homogeneous in size, it is necessary to use a living/controlled polymerization technique. Controlled radical polymerization (CRP) has enlarged the possibility of molecular weight control to a wide variety of monomers which could not be polymerized by living ionic polymerizations. Among the main CRP techniques, RAFT (reversible addition–fragmentation chain transfer)^{1–3} proved to be very versatile^{4,5} and efficient for a wide range of useful monomers.^{6–15}

RAFT polymerization is carried out in the presence of thiocarbonylthio compounds of general structure Z–C(=S)S–R that act as efficient reversible chain transfer agents (CTA) and result in the formation of end-functionalized polymer chains.¹⁶ RAFT polymerization of different monomers has been reported by several groups in both organic and aqueous media using a variety of CTA: xanthates (dithiocarbonates),^{17,18} dithiocarbamates,^{19–22} trithiocarbonates,^{23–27} and dithioesters.^{28–30}

One promising application of RAFT is the synthesis of highly fluorescent³¹ or light harvesting polymers³² by introducing photoactive moieties in a chain with low polydispersity and controlled molecular weight. However, many authors have found that the fluorescence of dyes attached to polymers obtained by RAFT is strongly quenched. This behavior was first reported by Chen et al. for polymers containing acenaphthyl energy donors and a terminal anthryl energy acceptor³² as well as for

linear and star-shaped light harvesting polymers with Ru(II) polypyridine energy trapping cores (from the CTA) and coumarin-2 derived monomer as light harvesting antennae.³³ Fluorescence quenching was also observed to lower the overall energy transfer efficiency in RAFT polymers containing acenaphthylene monomer units and coumarin (from the CTA),³⁴ with the fluorescence quenching being reduced by introducing a poly(acrylic acid) spacer between the poly(acenaphthylene) block and the coumarin chain end. In another study, a copolymer containing alternated acenaphthylene and maleic acid units with a terminal 9,10-diphenylanthryl energy acceptor showed an increase in energy transfer efficiency at low pH values.³⁵ Finally, in anthracene α -end-functionalized polystyrene chains synthesized by the RAFT process, the fluorescence intensity increased with the space between dye and dithioester chain end.³⁶ Despite all these results, to our knowledge, the mechanism of fluorescence quenching in polymers obtained by the RAFT process is not yet studied.

Here, we report the quenching of a coumarin dye fluorescence by several low molecular weight CTAs and one macroCTA. The low molecular weight CTAs, already used in RAFT polymerization,¹² are carboxymethyl dithiobenzoate (CMDDB), *tert*-butyl dithiobenzoate (*t*BDB), menthonyl dithiobenzoate (MDB), and bis(3-methylbutyl)-2-(thiobenzoylthio)succinate (MBTS) (Figure 1). All these dithioesters have the same Z group, a phenyl group, which ensures a high addition rate due to extensive intermediate radical stabilization.³⁷ They differ in the R group, which is primary for CMDDB, secondary for MBTS, and tertiary for *t*BDB and MDB.

The macroCTA results from the RAFT polymerization of *N*-decylacrylamide (DcA) in the presence of MBTS as chain transfer agent (poly(DcA)–MBTS, Figure 2). This short polymer chain ($M_n = 2940 \text{ g mol}^{-1}$) has been considered to evaluate

* To whom correspondence should be addressed: e-mail farinha@ist.utl.pt; Tel 351218419221.

[†] Instituto Superior Técnico.

[‡] École Normale Supérieure de Lyon.

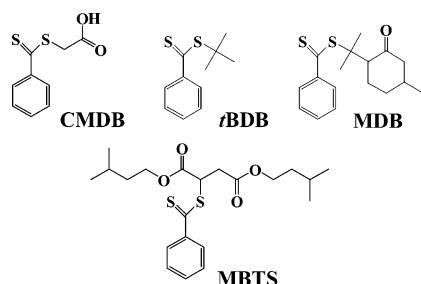


Figure 1. Structures of the dithiobenzoate RAFT chain transfer agents.

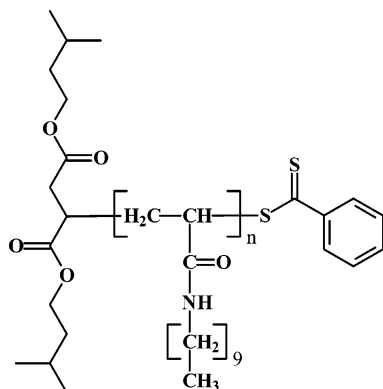


Figure 2. Structure of poly(DcA)-MBTS, $n = 12$.

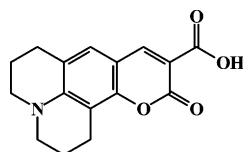


Figure 3. Structure of coumarin 343.

the effect of the monomer units introduced in between the dithiobenzoate group and the R group on the quenching of the dye.

We have chosen coumarin 343 (C343, Figure 3) for the fluorescence quenching experiments because this chromophore can be excited at wavelengths where the CTA absorption is relatively low, and it is soluble in the same solvents as the CTAs. Furthermore, C343 has a high fluorescence quantum yield and a single-exponential decay³⁸ because it does not have a nonradiative twisted intramolecular charge transfer (TICT) state in polar solvents, common in other coumarin dyes, since the rotation of the 7-amino group is hindered.³⁹

Both steady-state and time-resolved fluorescence studies have been carried out to compare the fluorescence quenching of coumarin by the various CTAs and the macroCTA. Furthermore, a kinetic model is proposed to describe the dye fluorescence quenching mechanism.

Finally, we checked if removing the thiocarbonylthio function would suppress the fluorescence quenching of the coumarin dye. As the thiocarbonylthio function is easily transformed into a thiol group in the presence of nucleophiles such as hydroxide ions and primary (or secondary) amines,^{22,23,40,41} two control experiments were performed. First, *tert*-butyl mercaptan (*t*BM) was used as a model for the aminolysis product of the low molecular weight CTA, *t*BDB. Second, aminolysis of the poly-(DcA)-MBTS macroCTA was carried out with hexylamine to obtain the thiol-terminated chain, poly(DcA)-SH. Both *t*BM and poly(DcA)-SH were tested as quenchers for the C343 fluorescence, using the same experimental conditions as for the corresponding CTA.

Experimental Section

Materials. Carboxymethyl dithiobenzoate (CMDB, Aldrich, 99%) and *tert*-butyl mercaptan (*t*BM, Aldrich, 99%) were used without further purification. 2,2'-Azobis(isobutyronitrile) (AIBN) (Fluka, 98%) was purified by recrystallization from ethanol, 1,4-dioxane (Acros, 99%) was distilled over LiAlH_4 (110 °C), and trioxane (Acros, 99%) was used as received. The synthesis of menthyl dithiobenzoate (MDB),¹² *tert*-butyl dithiobenzoate (*t*BDB),¹² and bis(3-methylbutyl)-2-(thiobenzoylethio)succinate (MBTS)⁴² has been previously described. All the dithioesters were stored under nitrogen in the dark at -10 °C. Coumarin 343 (C343, Aldrich, 97%) and acetone (Sigma-Aldrich, spectrophotometric grade) were used as received.

Synthesis of *N*-Decylacrylamide (DcA). DcA was synthesized by a classical amidation reaction between distilled acryloyl chloride (Aldrich, 96%) and *N*-decylamine (Aldrich, 95%) in dichloromethane (VWR) in the presence of triethylamine (Aldrich, 99.5%).⁴³ *N*-Decylamine (47.9 g, 0.289 mol) and triethylamine (32.4 g, 0.318 mol) were dissolved in 300 mL of dichloromethane in a 500 mL round-bottom flask with a stirring bar in an ice bath. Acryloyl chloride (29.0 g, 0.320 mol) was added dropwise over a period of 1.5 h, keeping the temperature below 2.5 °C. After stirring for an additional 30 min, the mixture was washed twice with saturated aqueous solutions of NH_4Cl , NaHCO_3 , and NaCl . The crude product was dried over anhydrous MgSO_4 and filtered, and the solvent was removed by evaporation. Finally, it was recrystallized four times from pentane at low temperature to recover white crystals of *N*-decylacrylamide by filtration, which were then dried under vacuum (70% yield).

Synthesis of Poly(DcA)-MBTS. Poly(DcA)-MBTS was obtained from the RAFT polymerization of DcA in the presence of MBTS as chain transfer agent. DcA (3.00 g, 14.2 mmol), MBTS (0.15 g, 0.38 mmol), AIBN (6.2 mg, 37.5 μmol), 1,4-dioxane (13.9 mL), and trioxane (0.11 g, internal reference for ^1H NMR determination of monomer consumption) were introduced in a Schlenk tube equipped with a magnetic stirrer. The mixture was degassed by four freeze-evacuate-thaw cycles and then heated under nitrogen in a thermostated oil bath (90 °C). Monomer conversion was determined by ^1H NMR spectroscopy using a Bruker AC 200 spectrometer (200 MHz), by comparison of one vinylic proton (5.6 ppm) with trioxane (5.1 ppm) used as internal reference.⁴⁴ Typically, 400 μL of *d*-chloroform was added to 200 μL of each sample. The polymer (obtained at 32% conversion) was precipitated in a large volume of cold DMSO, recovered by centrifugation, and finally dried under vacuum before analysis. The molecular weight of poly(DcA)-MBTS determined by MALDI-TOF mass spectrometry⁴¹ ($M_{\text{peak}} = 2760 \text{ g mol}^{-1}$) was close to the value expected from conversion data (2940 g mol^{-1}). The relative polydispersity index $M_w/M_n = 1.10$ was obtained from SEC in THF using polystyrene standards.⁴⁵

Sample Preparation. Solutions of C343 in acetone, with concentrations ranging from 10^{-4} to 10^{-7} M, were prepared from a 9.64×10^{-4} M stock solution. Stock solutions of the four CTA, macroCTA, and *t*BM were also prepared in acetone. Mixed solutions of each one of these compounds, with concentrations from 0 to ca. 2.5×10^{-2} M, and C343 (10^{-4} M) were prepared in the same day of fluorescence measurements to prevent degradation.

Instrumentation. UV-vis absorption measurements were performed in a Shimadzu UV-vis 3101PC spectrometer, and fluorescence spectra were recorded on a SPEX Fluorolog F112A fluorometer (bandwidths of 4.5 nm in excitation and 2.25 nm in emission). Emission spectra were recorded between 430 and 650 nm by excitation at 420 nm. The excitation spectra were recorded at the emission wavelength of 485 nm by scanning the excitation light from 300 to 480 nm. All spectra were obtained with right angle geometry, at room temperature using square quartz cells of 0.5 cm \times 0.5 cm.

Fluorescence intensity decay curves were obtained by the single-photon timing technique using picosecond laser excitation at 420 nm. The system consists of a mode-locked Coherent Inova 440-10

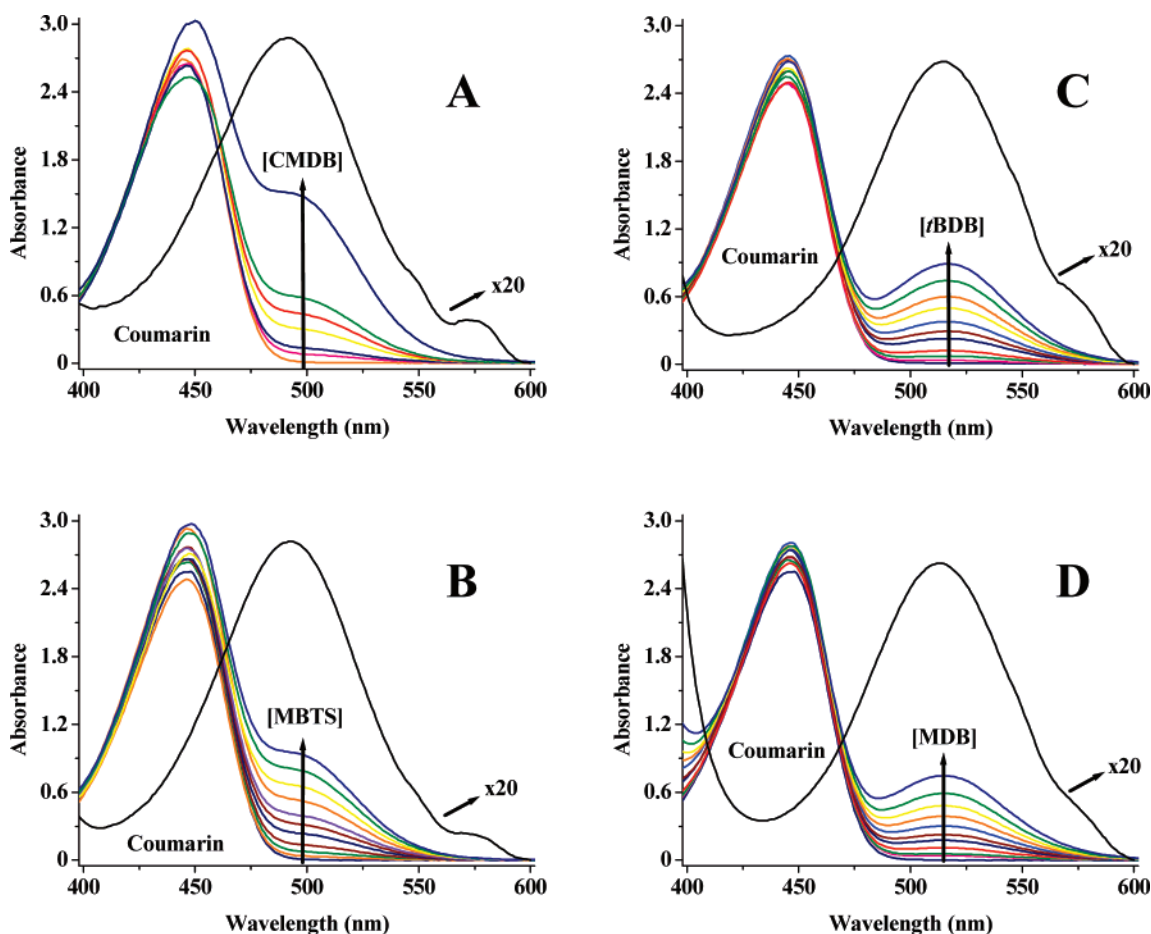


Figure 4. Absorption spectra of mixed solutions of C343 (10^{-4} M) and increasing concentrations (0 to ca. 0.025 M) of (A) CMDB, (B) MBTS, (C) *t*BDB, and (D) MDB, in acetone. The solid black lines correspond to a 20 \times amplification of the CTA absorption spectra.

argon ion laser synchronously pumping a cavity dumped Coherent 701-2 dye laser using DCM, which delivers 5–6 ps pulses at a repetition rate of 460 kHz. The excitation light frequency was doubled using a BBO crystal. The fluorescence was observed at 485 nm using a polarizer at the magic angle, being the scattered light effectively eliminated by a cutoff filter. The fluorescence was selected by a Jobin-Yvon HR320 monochromator with a 100 lines/mm grating and detected by a Hamamatsu 2809U-01 microchannel plate photomultiplier. The fluorescence decay curves were analyzed by a nonlinear least-square reconvolution method^{46,47} based on the Marquard algorithm.⁴⁸ All measurements were performed at room temperature.

Results and Discussion

The thiocarbonylthio compounds used as chain transfer agents (CTA) in RAFT polymerization have a structure of the type $Z-C(=S)S-R$, with different R and Z groups. In order to characterize the strong fluorescence quenching observed on dyes attached to polymer chains synthesized by the RAFT process, we chose four different dithiobenzoates: CMDB, MBTS, *t*BDB, and MDB (Figure 1). Their absorption spectra in acetone (Figure 4) show that CMDB and MBTS have similar absorbance bands with maxima at 490 nm, while *t*BDB and MDB have absorbance maxima at ca. 512 nm. All the CTA are nonfluorescent.

We chose the fluorescent dye coumarin 343 (C343, Figure 3) because its absorption spectra do not overlap with the absorption bands of the CTAs and therefore can be selectively excited in the CTA absorption minimum, around 420 nm (Figure 4). In addition, C343 is very soluble in acetone, a good solvent for the CTA compounds used in the present study. For a wide range of concentrations in acetone (10^{-7} – 10^{-4} M), C343 shows

no change in the spectra shape, with an absorption maximum at 445 nm and a molar absorption coefficient of $38\,000\text{ M}^{-1}\text{ cm}^{-1}$, whereas its fluorescence spectra show a broad band centered at 488 nm (Figure 5).

Another useful characteristic of C343 is that it has monoexponential fluorescence decays in a wide range of concentrations in acetone. Time-resolved fluorescence decay curves of 10^{-7} – 10^{-4} M solutions of C343 in acetone could be fitted with a single-exponential function, with a lifetime of $\tau = 4\text{ ns}$ (homogeneously distributed weighted residuals and autocorrelation of the residuals and $\chi^2 < 1.1$ were obtained for all experiments).

The CTA concentration range used in the experiments corresponds to extreme conditions of high CTA/dye concentration ratio, which can be found for example in polymer samples of low molecular weight with a dithioester (DT) group at the chain end, and a low amount of fluorescent dye (as is usually the case when the dyes are used as reporter groups). Although in polymers obtained by the RAFT process there is usually only one DT group per chain, the local effective DT concentration around a dye can be quite high, since the chain conformation can force the DT and the dye to be separated by short distances. To mimic the local DT concentration, it was assumed that the radius of the sphere where the DT is located is ca. 3–12 nm, which corresponds to the typical hydrodynamic radius of polymers obtained by RAFT.

The absorption spectra of the mixed solutions of CMDB, *t*BDB, MBTS, and MDB (from 0 M up to ca. 0.025 M) with C343 (10^{-4} M) in acetone correspond to the sum of the CTA and C343 absorption bands (Figure 4). Regarding the fluores-

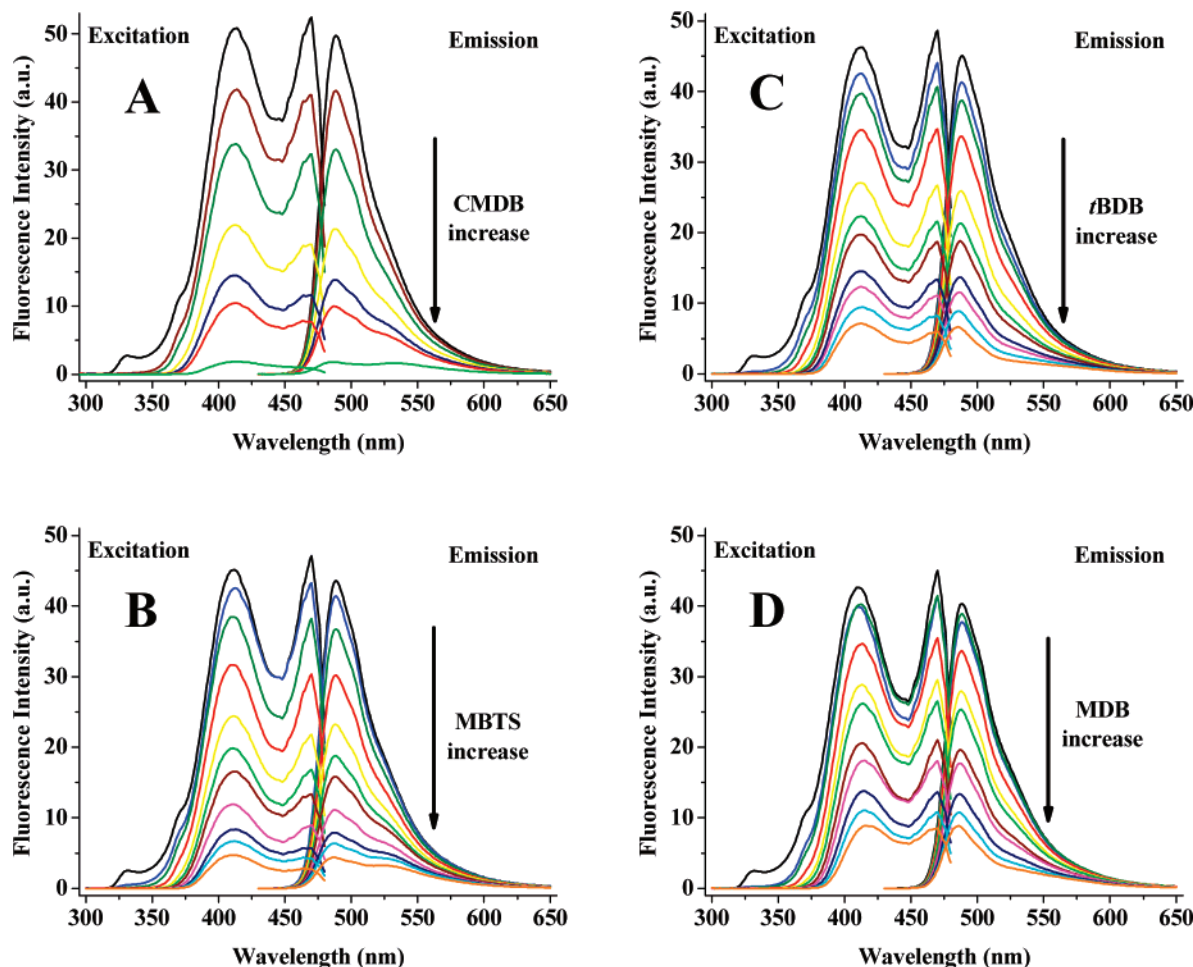


Figure 5. Fluorescence emission ($\lambda_{\text{ex}} = 420$ nm) and excitation ($\lambda_{\text{em}} = 485$ nm) spectra of mixed solutions of 10^{-4} M coumarin 343 and increasing concentrations (0 to ca. 0.025 M) of (A) CMDB, (B) MBTS, (C) *t*BDB, and (D) MDB, in acetone.

cence of C343, both the emission ($\lambda_{\text{ex}} = 420$ nm) and excitation spectra ($\lambda_{\text{em}} = 485$ nm) show an intensity decrease with the increase of the dithioester concentration (Figure 5), accompanied by a change in the shape of the fluorescence spectra for all the C343–CTA mixed solutions. The decrease in intensity observed around 470 nm in the excitation spectra is due to the absorption of the CTAs in this wavelength range.

The superposition of the dithioester absorption (Figure 4) and the C343 fluorescence emission (Figure 5) suggests the possibility of energy transfer from C343 to the dithioesters. However, the efficiency of energy transfer should be extremely low because the superposition integrals of C343 emission and dithioester absorption are very small (the molar absorption coefficients of the dithioesters are very low, $\epsilon < 100 \text{ M}^{-1} \text{ cm}^{-1}$), and therefore this process is not expected to affect the intrinsic lifetime of C343.

The change in the shape of the emission spectra is due to a new band, with maximum around 530 nm for CMDB and MBTS and 550 nm for *t*BDB and MDB. This new emission was attributed to the formation of an emissive charge transfer complex (exciplex) between the dye and the CTA, resulting from electron transfer from the excited coumarin to the CTA, which is a good electron acceptor.

The C343–CTA exciplex emission can be readily observed by subtracting the fluorescence intensity of C343 from the fluorescence intensity of the dye in the presence of CTA, both normalized at their maxima (Figure 6). In the case of CMDB and MBTS, the exciplex band is centered at ca. 533 nm, being red-shifted by ca. 5 nm with the increased in CTA concentration.

For *t*BDB and MDB the exciplex band is closer to the emission of C343 and therefore appears only as a shoulder centered at 555 nm for low CTA concentrations. This band increases with the CTA concentration and is red-shifted by ca. 15 nm. The inversion points observed for C343–*t*BDB at 545 nm and C343–MDB at 540 nm (Figure 6) result from the decrease in C343 emission caused by the absorption of the CTA (Figure 4).

The C343–CTA exciplex probably results from the diffusional encounter of the excited dye with the CTA, and therefore the quenching of the C343 fluorescence would be described by a Stern–Volmer equation⁴⁹

$$\frac{F_0}{F} = 1 + k_q \tau_0 [\text{CTA}] = 1 + K_D [\text{CTA}] \quad (1)$$

where F_0 and F are the fluorescence intensities in the absence and presence of the CTA quencher, k_q is the bimolecular quenching constant, and τ_0 is the lifetime of the C343 in the absence of CTA. In the absence of a ground-state complex and transient effects, the plot of F_0/F with $[\text{CTA}]$ would be linear.⁵⁰ The upward curvature, concave toward the y-axis (Figure 7A), indicates that the quenching process is not exclusively dynamic. If we consider the possibility of formation of a ground-state complex between the dye and the CTA with an equilibrium constant K_S , then⁴⁹

$$\frac{F_0}{F} = 1 + (K_D + K_S)[\text{CTA}] + K_D K_S [\text{CTA}]^2 \quad (2)$$

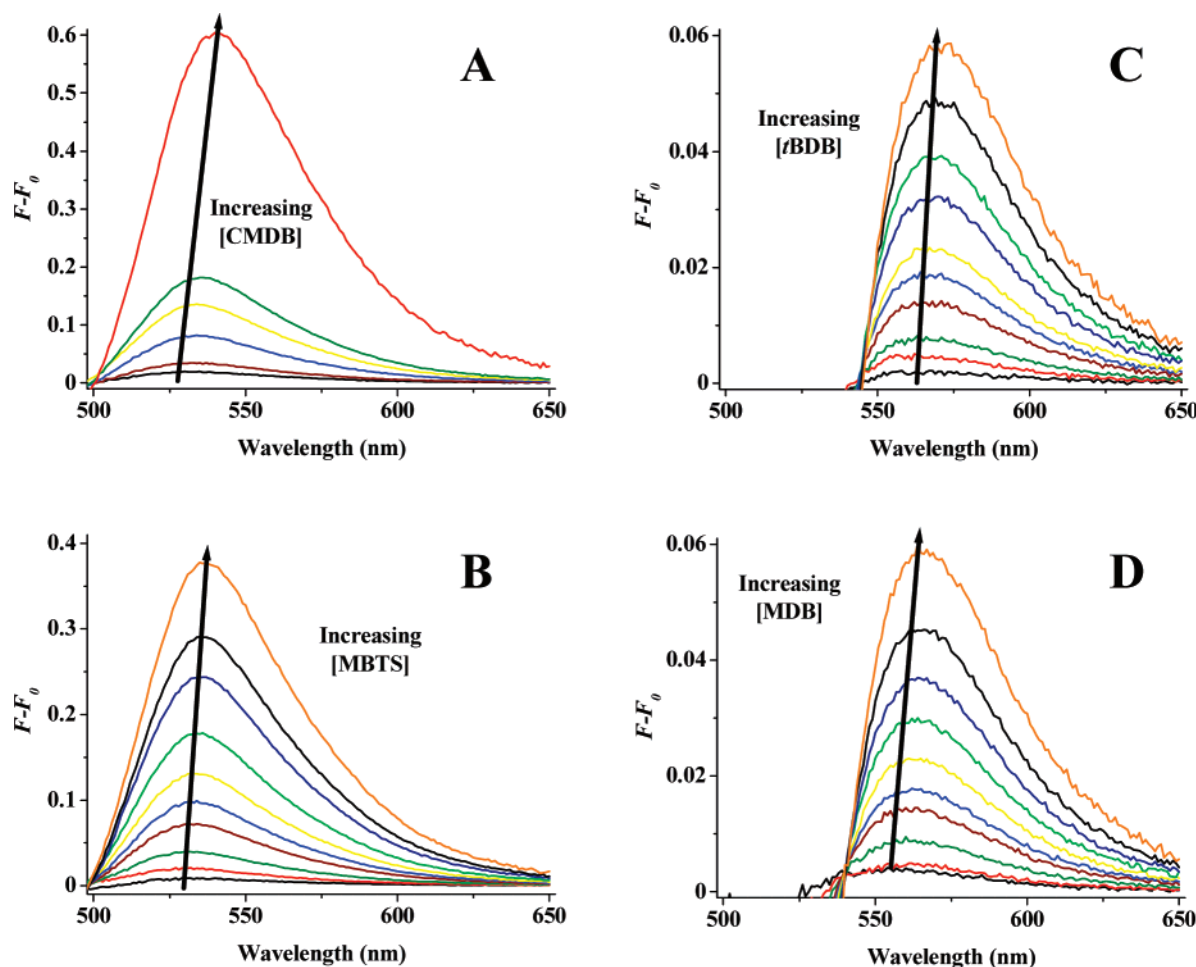


Figure 6. Fluorescence emission spectra ($\lambda_{\text{ex}} = 420$ nm) of C343-CTA complexes for CMDB (A), MBTS (B), *t*BDB (C), and MDB (D), in acetone.

which predicts that the plot of $(F_0/F - 1)/[\text{CTA}]$ with $[\text{CTA}]$ should be linear. However, a positive deviation from linearity is still observed (Figure 7B), suggesting a more complex quenching mechanism.

In order to better understand the quenching mechanism, we measured the time-resolved fluorescence intensity decays of 10^{-4} M C343 solutions for 0 to ca. 0.025 M of CTA in acetone (Figure 8). The C343 fluorescence decay becomes faster with the increase in CTA concentration, as expected. The fluorescence decay curve of C343 alone can be fitted with a single exponential function. However, in the presence of CTA the fluorescence decays could only be fitted with a sum of two exponential functions:

$$I_D(t) = A_1 \exp\left(-\frac{t}{\tau_1}\right) + A_2 \exp\left(-\frac{t}{\tau_2}\right) \quad (3)$$

The fluorescence lifetimes (τ_1 , τ_2) and preexponential factors (A_1 , A_2) were obtained by fitting the fluorescence intensity decay curves of mixed solutions of C343 (10^{-4} M, in acetone) with CMDB, *t*BDB, MDB, and MBTS by excitation at 420 nm and detection at 485 nm (Figure 8). The decays recorded at 500, 530, and 550 nm (in the region of the C343-CTA complex emission, Figure 6) show identical lifetimes and slightly different preexponential coefficients. This indicates that the excited C343 and the exciplex are in equilibrium,⁵¹ thus explaining the failure to obtain a linear relation in Figure 7.

Quenching Kinetics. To understand the quenching mechanism of C343 by the CTA, we have to take into account the

existence of a C343-CTA ground-state complex in equilibrium with C343. We consider a fluorophore C and a quencher CTA that can associate reversibly in the ground state as C-CTA with equilibrium constant K . Both C and C-CTA can be directly excited to give C^* and the exciplex E^* by absorption of a fraction of light α and $1 - \alpha$, respectively. The exciplex E^* can also be formed by the encounter of C^* and CTA with rate constant k_1 and can dissociate with rate constant k_{-1} . This model is represented in Scheme 1, where τ_C is the lifetime of C^* and τ_E is the lifetime of the exciplex, E^* .

According to Scheme 1, the time evolution of the concentrations of the species C^* and E^* are described by the following differential equations:

$$\frac{d[C^*]}{dt} = \alpha I_0 + k_{-1}[E^*] - \left(k_1[\text{CTA}] + \frac{1}{\tau_M}\right)[C^*] \quad (4)$$

$$\frac{d[E^*]}{dt} = (1 - \alpha)I_0 + k_1[C^*][\text{CTA}] - \left(k_{-1} + \frac{1}{\tau_{\text{MQ}}}\right)[E^*] \quad (5)$$

Under photostationary conditions, since $F_C(t) \propto [C^*]$ and $F_E(t) \propto [E^*]$, we obtain the Stern-Volmer type expression for C343 emission quenching

$$\frac{F_0}{F} = \left\{ \frac{k_{-1}\tau_E + 1}{\alpha + k_{-1}\tau_E} + \frac{k_1\tau_C}{\alpha + k_{-1}\tau_E}[\text{CTA}] \right\} (1 + K[\text{CTA}]) \quad (6)$$

which rearranges to

$$\frac{F_0}{F} = \gamma_1 + (\gamma_1 K + \gamma_2)[CTA] + \gamma_2 K[CTA]^2 \quad (7)$$

with

$$\gamma_1 = \frac{k_{-1}\tau_E + 1}{\alpha + k_{-1}\tau_E} \quad (8a)$$

$$\gamma_2 = \frac{k_1\tau_C}{\alpha + k_{-1}\tau_E} \quad (8b)$$

Equation 7 predicts dynamic plus static quenching described by eq 2 only if all the excitation light is absorbed by the coumarin ($\alpha = 1$) and the exciplex formation is irreversible ($k_{-1} = 0$).

Equations 4 and 5 can be solved for a δ pulse of excitation light to yield

$$[C^*] = a_1^C e^{-t/\tau_1} + a_2^C e^{-t/\tau_2} \quad (9)$$

$$[E^*] = a_1^E e^{-t/\tau_1} + a_2^E e^{-t/\tau_2} \quad (10)$$

with the kinetic parameters given by

$$1/\tau_1 = \lambda_1 = \frac{-(A+B) + \sqrt{(A-B)^2 + 4k_{-1}k_1[CTA]}}{2} \quad (11)$$

$$1/\tau_2 = \lambda_2 = \frac{-(A+B) - \sqrt{(A-B)^2 + 4k_{-1}k_1[CTA]}}{2} \quad (12)$$

$$a_1^C = \frac{\lambda_1 + B}{\lambda_1 - \lambda_2} [C^*]^0 - \frac{(\lambda_1 + B)(\lambda_2 + B)}{k_1(\lambda_1 - \lambda_2)} [E^*]^0 \quad (13)$$

$$a_2^C = \frac{\lambda_2 + B}{\lambda_1 - \lambda_2} [C^*]^0 + \frac{(\lambda_1 + B)(\lambda_2 + B)}{k_1(\lambda_1 - \lambda_2)} [E^*]^0 \quad (14)$$

$$a_1^E = \frac{k_1}{\lambda_1 - \lambda_2} [C^*]^0 - \frac{\lambda_2 + B}{\lambda_1 - \lambda_2} [E^*]^0 \quad (15)$$

$$a_2^E = \frac{k_1}{\lambda_1 - \lambda_2} [C^*]^0 - \frac{\lambda_1 + B}{\lambda_1 - \lambda_2} [E^*]^0 \quad (16)$$

with

$$A = k_1[CTA] + \frac{1}{\tau_C} \quad (17)$$

$$B = k_{-1} + \frac{1}{\tau_E} \quad (18)$$

and $[C^*]^0$, $[E^*]^0$ being the initial concentrations of excited dye and complex produced by a δ -pulse of excitation light.

Since the lifetime of C343 was determined independently ($\tau_C = 4.04$ ns), it was possible to determine the quenching constant, k_1 , by relating the expressions of the decay lifetimes τ_1 , τ_2

$$\frac{1}{\tau_1} + \frac{1}{\tau_2} = \left(\frac{1}{\tau_C} + \frac{1}{\tau_E} + k_{-1} \right) + k_1[CTA] \quad (19)$$

On the other hand, combining eqs 11 and 12 in a different way,

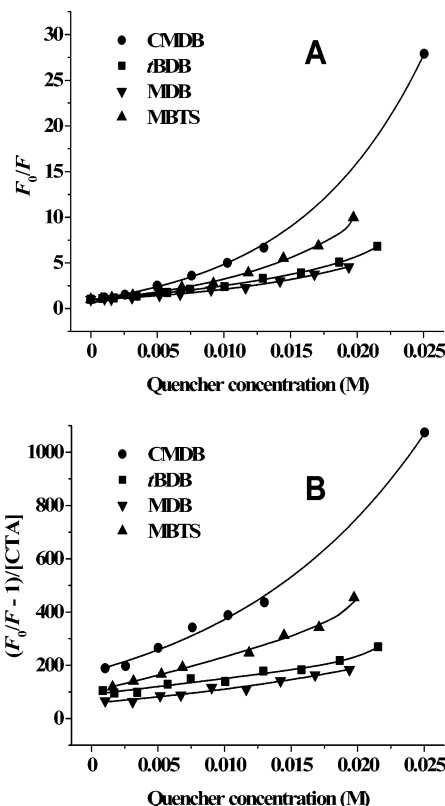


Figure 7. Quenching of C343 (10^{-4} M in acetone, excited at 420 nm) by CMDB (●), tBDB (■), MDB (▼), and MBTS (▲) is not described by a Stern–Volmer (A) or a simultaneous static and dynamic quenching (B), as indicated by the nonlinear plots.

we obtain a new expression from which we calculate τ_E and k_{-1}

$$\frac{\tau_C}{\tau_1\tau_2} = \left(\frac{1}{\tau_E} + k_{-1} \right) + \left(\frac{k_1\tau_C}{\tau_E} \right) [CTA] \quad (20)$$

In Figure 9, we show the linear plots predicted by eqs 19 and 20 for the data in Figure 8. The model parameters recovered from fitting the data with these expressions are shown in Table 1.

Using the experimental values of F_0/F and the kinetic parameters determined with eqs 19 and 20, it was possible to determine the ground state equilibrium constant K and the ratio of molar absorption coefficients of the complex and the dye, $r_e = \epsilon_E/\epsilon_C$, using eq 7 and

$$\alpha = \frac{\epsilon_C[C]}{\epsilon_C[C] + \epsilon_E[E]} = \frac{1}{1 + \frac{\epsilon_E}{\epsilon_C} K[CTA]} \quad (21)$$

In Figure 10, the theoretical and experimental F_0/F ratios are shown for the four dye/CTA systems, with the parameters recovered presented in Table 1.

Using the kinetic parameters calculated from the reversible quenching model (Table 1), we calculated the decay parameters τ_1 , τ_2 , A_1 , and A_2 . The results are in good agreement with the experimental values (Figure 11), indicating that the dye fluorescence quenching mechanism by the various CTAs is well described by the proposed kinetic scheme, reflecting a reversible association between coumarin and CTA in the ground state as well as an equilibrium between the electronically excited dye and the CTA–coumarin exciplex. Furthermore, the quenching mechanism is the same for all the CTAs tested, indicating that

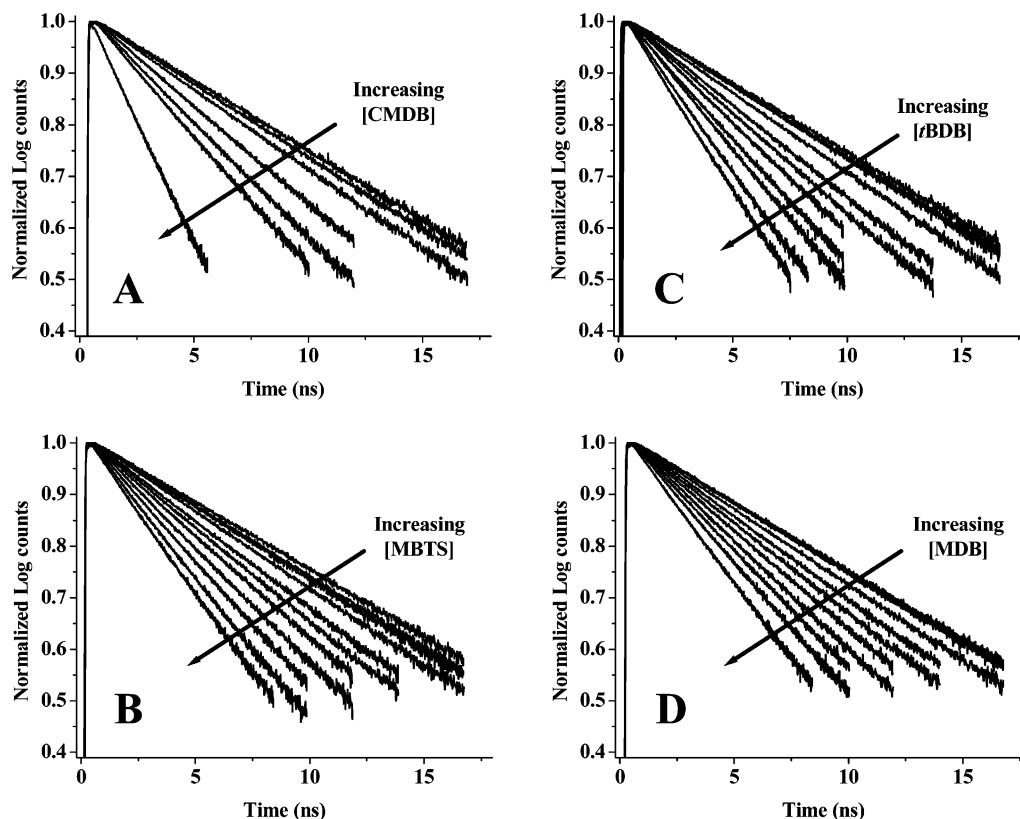
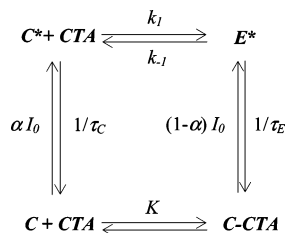


Figure 8. Normalized fluorescence emission decay curves obtained at 485 nm for the mixed solutions of 10^{-4} M C343 and increasing concentrations (0 to ca. 0.025 M) of (A) CMDB, (B) MBTS, (C) *t*BDB, and (D) MDB, in acetone, by excitation at 420 nm.

Scheme 1. Kinetic Model for Reversible Static and Dynamic Quenching



the nature and/or structure of the R group, whether primary, secondary, or tertiary, have little influence on the quenching effect of these dithiobenzoates, which is apparently governed by the thiocarbonylthio function.

In order to test whether the quenching model was still valid for a macroCTA, we applied it to the quenching of C343 by a poly(DcA)–MBTS chain resulting from the RAFT polymerization of *N*-decylacrylamide (DcA) using MBTS as chain transfer agent.

The hydrophobic poly(DcA) chain have an average of 12 monomer units separating the dithiobenzoyl group from the R group of MBTS. Steady-state and time-resolved fluorescence measurements were performed using the same experimental conditions as for the low molecular weight CTAs. Increasing amounts of poly(DcA)–MBTS (0 to 0.0187 M) were added to the C343 (10^{-4} M) in acetone. The fluorescence spectra ($\lambda_{\text{ex}} = 420$ nm) of the dye and macroCTA mixed solutions are shown in Figure 12. An exciplex with emission band also at ca. 530 nm is formed (Figure 12, inset), and the decrease in C343 fluorescence intensity with the increase in poly(DcA)–MBTS concentration is similar to that induced by the corresponding low molecular weight CTA, MBTS. Also, the time-resolved picosecond fluorescence decay curves of 10^{-4} M C343 in

acetone (excitation at 420 nm and emission monitored at 485 nm) are similar to those obtained in the presence of equal amounts of poly(DcA)–MBTS and MBTS.

Although in poly(DcA)–MBTS the functional group responsible for the fluorophore quenching is attached to the polymer chain and therefore should diffuse slowly, it does not show significant differences from what was observed for the smaller CTAs. The similarity between the macroCTA and MBTS probably results from the small size of the poly(DcA)–MBTS chain and its affinity toward acetone. In a more detailed comparison between the quenchers, one can say that the decrease in the C343 emission was slightly smaller for the macroCTA. This difference might be explained by the usually small amount of polymer chains that are not ended by a dithioester function in RAFT polymerization. With the experimental conditions chosen to perform this polymerization, it is expected that ca. 9 mol % of poly(DcA) chains do not have a dithioester end group (dead chains).^{15,41} The elimination of these chains is practically impossible during polymer purification. These polymer chains do not quench C343, leading to the slightly smaller quenching effect observed for poly(DcA)–MBTS as compared with MBTS.

The kinetic model described earlier was used to analyze the quenching of C343 by the macroCTA. From the plot of $(1/\tau_1 + 1/\tau_2)$, $(\tau_C/\tau_1\tau_2)$, and F_0/F for poly(DcA)–MBTS (eqs 7, 19, and 20), we obtained the kinetic parameters (Table 1, Figure 13). The experimental decay parameters τ_1 , τ_2 , A_1 , and A_2 obtained for the C343 quenching by poly(DcA)–MBTS are well reproduced by those calculated theoretically using the kinetic parameters obtained from eqs 11–18 (Figure 14).

Although the results obtained with the four low molecular weight CTAs and the macroCTA could be described by the same kinetic model, there are some differences in the parameters calculated for the different CTAs. First, the lifetimes of the

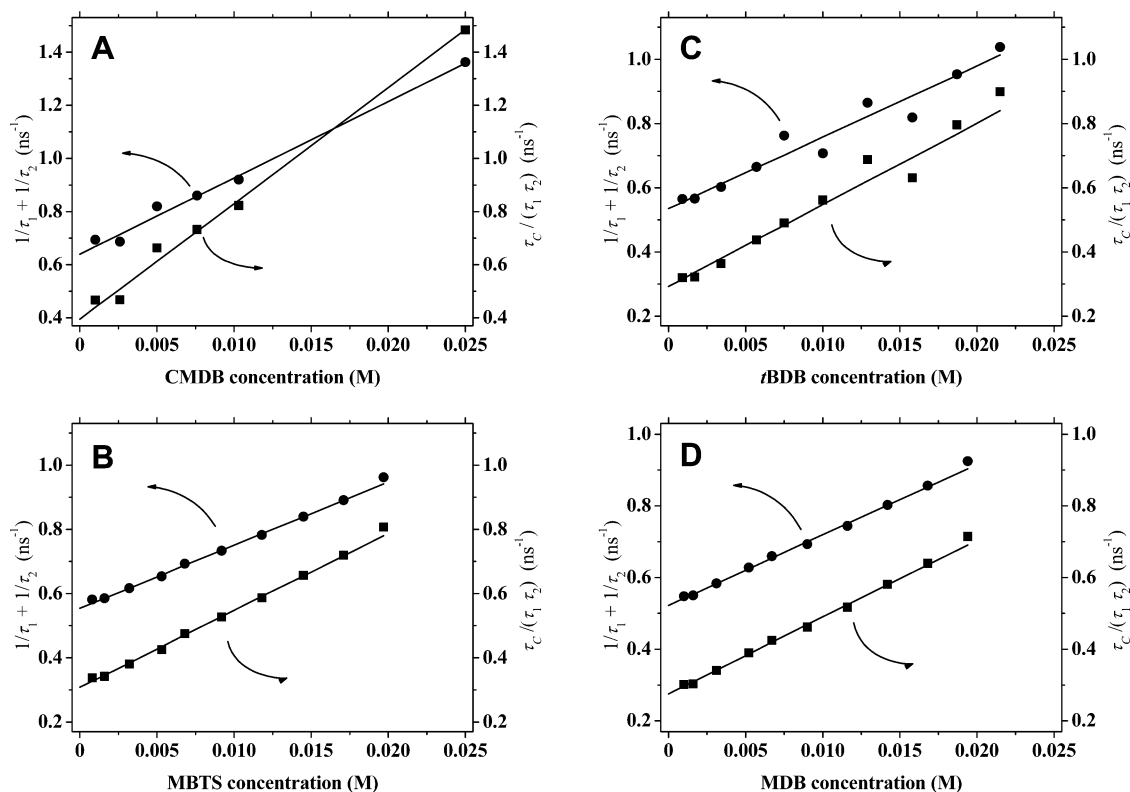


Figure 9. Plot of $(1/\tau_1 + 1/\tau_2)$ and $(\tau_c/\tau_1\tau_2)$ vs the quencher concentration for (A) CMDB, (B) MBTS, (C) *t*BDB, and (D) MDB, using the data in Figure 8.

Table 1. Kinetic Parameters for the Reversible Quenching Process of C343 by Different CTA

CTA	τ_E (ns)	$r_e = \epsilon_E/\epsilon_M$	k_1 ($M^{-1} ns^{-1}$)	k_{-1} (ns^{-1})	K (M^{-1})
CMDB	2.7	0.97	29	0.02	53
<i>t</i> BDB	3.5	0.95	22	0.01	20
MDB	3.7	0.97	20	0.01	16
MBTS	3.3	0.97	20	0.01	43
poly(DcA)–MBTS	3.9	0.89	16	0.01	57

C343–CTA excited complexes (τ_E) increase from primary CTA (S atom is connected to a primary C atom in the R group), CMDB, to secondary CTA, MBTS, to tertiary CTAs, *t*BDB and MDB, with the macroCTA, poly(DcA)–MBTS, showing a larger exciplex lifetime possibly due to its slower dynamics (much larger size). Second, we obtained values of k_1 on the order of $10^{10} M^{-1} s^{-1}$, typical of diffusion-controlled processes. This means that the quenching process is very efficient. In fact,

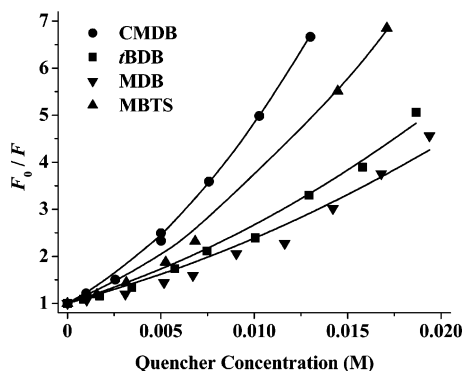


Figure 10. Steady-state modified Stern–Volmer plots (reversible quenching mechanism) for 10^{-4} M C343 with CMDB (●), *t*BDB (■), MDB (▼), and MBTS (▲) in acetone. Experimental values are represented by full symbols, and the solid lines are calculated with the parameters recovered using the proposed kinetic model.

we notice that the value of the quenching constant k_1 is smaller for larger molecules, an indication that the quenching process is effectively diffusion-controlled. The smaller chain transfer agents, CMDB and *t*BDB, have the higher quenching constant, while the macroCTA presents the lowest k_1 value. As for the dissociation rate constant, k_{-1} , the values can only be obtained with a large associated error. Nevertheless, we observed that the k_{-1} values are similar for all CTA. Finally, the values obtained for the ground-state equilibrium constant K show that there is less dye–CTA preassociation for the tertiary CTAs, *t*BDB and MDB, as compared with the secondary CTAs, MBTS and poly(DcA)–MBTS, and the primary CTA, CMDB.

Eliminating Fluorescence Quenching in Polymers Obtained by the RAFT Process. We have shown that the quenching of fluorescence in polymers synthesized by RAFT polymerization is due to the thiocarbonylthio function of the CTA. In the case of the coumarin dye, C343, and presumably for similar fluorescent dyes, such quenching involves the formation of a CTA–dye complex, which is in equilibrium with the dye both in the ground state and in the excited state. In view of the numerous advantages of using RAFT polymerization to prepare fluorescent polymers (low polydispersity, controlled molecular weight and dye content, and choice of different architectures for a wide range of monomers), it is of major importance to avoid the effects of fluorescence quenching in polymers obtained by the RAFT process. This can be accomplished by modifying the dithioester group into another group that does not quench the dye fluorescence. One way to do this is to convert the dithioester end group into a more stable thioether function through aminolysis and Michael addition to form α,β -unsaturated carbonyl derivatives.⁵² However, we found that a simpler procedure to eliminate quenching by the dithioester group was by aminolysis into a thiol group. Nakayama and Okano confirmed reliable aminolysis of the terminal

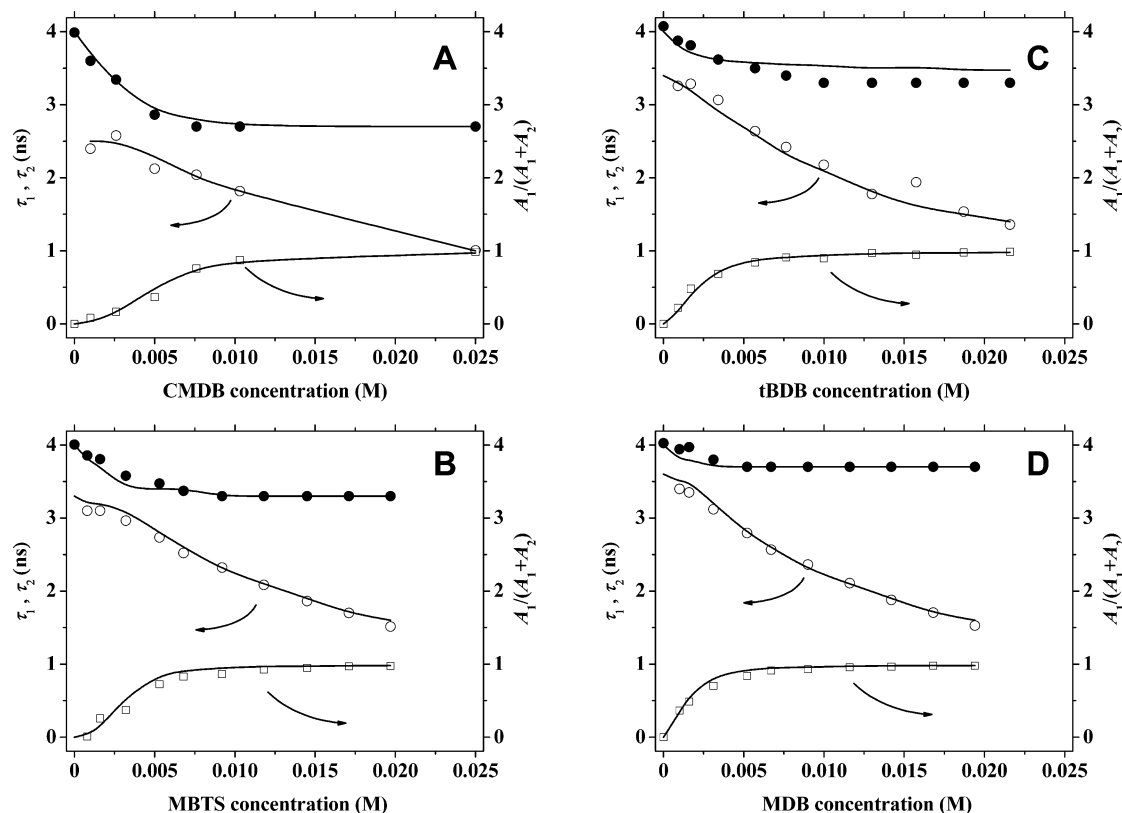


Figure 11. Lifetimes, τ_1 (open circles) and τ_2 (full circles), and preexponential factors, $A_1/(A_1 + A_2)$, obtained at 485 nm for the mixed solutions of 10^{-4} M C343 and increasing concentrations (0 to ca. 0.025 M) of (A) CMDB, (B) MBTS, (C) *t*BDB, and (D) MDB, in acetone, by excitation at 420 nm. Solid lines represent the values calculated using the kinetic parameters of Table 1 and eqs 11–14.

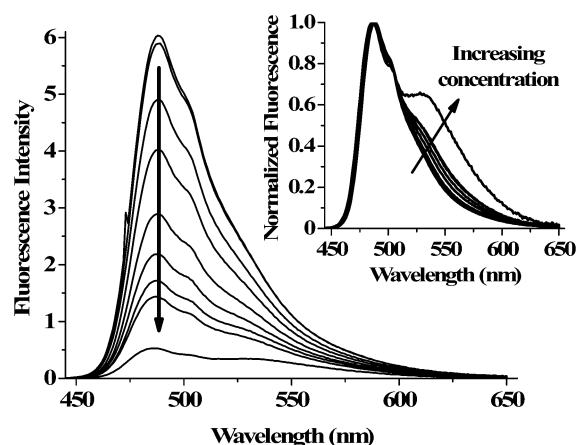


Figure 12. Fluorescence emission spectra ($\lambda_{\text{ex}} = 420$ nm) of mixed solutions of 10^{-4} M C343 and increasing concentrations of poly(DcA)–MBTS (0 to ca. 0.0187 M), in acetone. The emission spectra normalized at the intensity maximum (~ 490 nm) are shown in the inset.

dithiobenzoate group in polymers obtained by RAFT by the disappearance of both the $n-\pi^*$ dithiobenzoate absorption band around 500 nm and the 7.4–7.9 ppm ^1H NMR resonances.⁵³ Here, we used *tert*-butyl mercaptan (*t*BM) as a model for the aminolysis of *t*BDB in order to confirm that the thiol group does not act as a quencher.

Using the same experimental conditions as for *t*BDB, we mixed *t*BM (0–0.022 M) with 10^{-4} M C343 in acetone and measured the fluorescence emission ($\lambda_{\text{ex}} = 420$ nm) and excitation ($\lambda_{\text{em}} = 485$ nm) spectra as well as the time-resolved fluorescence intensity decays (excitation at 420 nm and emission monitored at 485 nm). In these experiments we did not observe any fluorescence decrease in the presence of *t*BM, and the fluorescence decay curves were monoexponential for all *t*BM

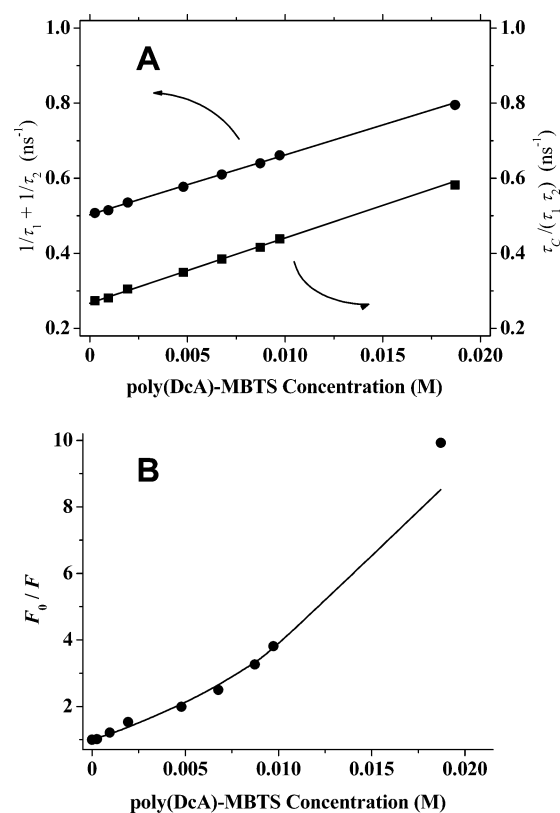


Figure 13. Plot of $1/\tau_1 + 1/\tau_2$ and $(\tau_c/\tau_1\tau_2)$ for 10^{-4} M C343 and poly(DcA)–MBTS in acetone (A) and modified Stern–Volmer reversible quenching mechanism (B).

concentrations. These results confirm that the thiol function does not act as a quencher of C343 fluorescence emission.

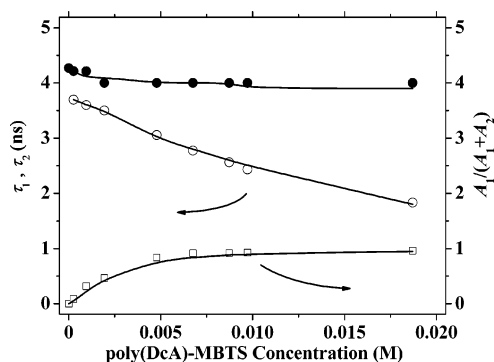


Figure 14. Experimental and calculated values of the lifetimes and preexponential factors of mixed solutions of 10^{-4} M C343 and increasing concentrations (0 to ca. 0.020 M) of poly(DcA)–MBTS, in acetone (emission at 485 nm and excitation at 420 nm).

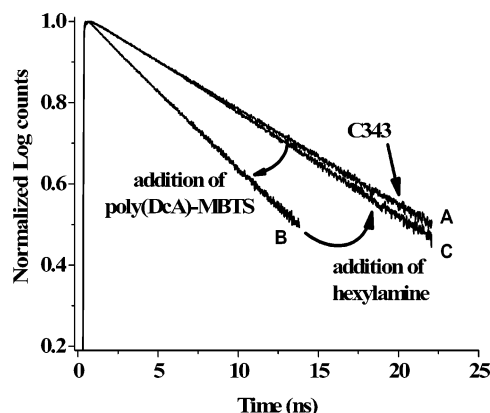


Figure 15. Normalized fluorescence emission decay curves obtained at 485 nm for 10^{-4} M C343 (A), after 0.972×10^{-2} M poly(DcA)–MBTS was added to the solution (B) and following addition of hexylamine (C).

We then applied this method to a mixed solution of 10^{-4} M C343 and 0.00972 M poly(DcA)–MBTS in acetone, using an excess of hexylamine. The reaction was performed at room temperature, in the dark and with magnetic stirring for 2–3 h. The final polymer was not purified, and fluorescent measurements were performed right after the reaction.

The decay curves, obtained with excitation at 420 nm and emission set at 485 nm (Figure 15), show that while the addition of poly(DcA)–MBTS macroCTA to a solution of C343 in acetone strongly decreases the dye lifetime, after conversion of the dithioester into a thiol, the C343 emission recovers to almost the same intensity as observed in the absence of macroCTA.

Conclusions

Reversible addition–fragmentation chain transfer (RAFT) polymerization can be used to obtain polymers with very good control of molecular weight and various architectures from a huge variety of monomers. These characteristics of RAFT polymerization are highly attractive for the synthesis of fluorescent polymers for a wide variety of applications. However, the dithiocarbonyl compounds used in the RAFT process as chain transfer agents (CTA) act as very efficient fluorescence quenchers. For the four CTAs and the macroCTA tested in this study, we found that the fluorescence quenching of the dye coumarin 343 (C343) occurs by the same reversible quenching mechanism, with formation of a CTA–C343 exciplex. The C343 time-resolved fluorescence measurements obtained at different wavelengths (485, 500, 530, and 550 nm) yielded similar decay times τ_1, τ_2 as expected from the kinetic model,

with slightly different preexponential factors in agreement with the small amount of exciplex emission observed in the fluorescence spectra. Analysis of the fluorescence decay curves obtained for C343 in the presence of different amounts of the CTAs with the proposed kinetic model proved that the quenching of C343 by the four low molecular weight CTAs and the macroCTA could be described by the same mechanism, with only minor differences in the parameters calculated for the different CTAs.

The aminolysis of the dithioester end group of a polymer chain synthesized by the RAFT process, leading to a thiol-ended chain, proved to be an efficient method to suppress the quenching of the coumarin C343 fluorescence. Moreover, the –SH end group can be further used to functionalize the polymer chain, for example attaching a biomolecule.³¹

Acknowledgment. We thank EGIDE/ICCTI (project 430 B3) and FCT (project POCTI/QUI/47885) for financial support. Paula Relógio acknowledges FCT for PhD grant SFRH/BD/1224/2000. We thank Dr. Alexander Fedorov for the fluorescence decay curve measurements and Dr. Arnaud Favier for the synthesis of *t*BDB, MDB, and MBTS.

References and Notes

- Chiefari, J.; Chong, Y. K.; Ercole, F.; Krstina, J.; Jeffery, J.; Le, T. P. T.; Mayadunne, R. T. A.; Meijs, G. F.; Moad, C. L.; Moad, G.; Rizzardo, E.; Thang, S. H. *Macromolecules* **1998**, *31*, 5559.
- Le, T. P. T.; Moad, G.; Rizzardo, E.; Thang, S. H. WO 9801478 A1 980115.
- Moad, G.; Chiefari, J.; Chong, B. Y. K.; Krstina, J.; Mayadunne, R. T. A.; Postma, A.; Rizzardo, E.; Thang, S. H. *Polym. Int.* **2000**, *49*, 993.
- Chong, Y. K.; Le, T. P. T.; Moad, G.; Rizzardo, E.; Thang, S. H. *Macromolecules* **1999**, *32*, 2071.
- Rizzardo, E.; Chiefari, J.; Mayadunne, R. T. A. In *Controlled/Living Radical Polymerization—Progress in ATRP, NMP, and RAFT*; ACS Symposium Series 768; Matyjaszewski, K., Ed.; American Chemical Society: Washington, DC, 2000; Vol. 768, p 278.
- Ganachaud, F.; Monteiro, M. J.; Gilbert, R. G.; Dourges, M.-A.; Thang, S. H.; Rizzardo, E. *Macromolecules* **2000**, *33*, 6738.
- Sumerlin, B. S.; Donovan, M. S.; Mitsukami, Y.; Lowe, A. B.; McCormick, C. L. *Macromolecules* **2001**, *34*, 6561.
- Baum, M.; Brittain, W. J. *Macromolecules* **2002**, *35*, 610.
- Donovan, M. S.; Lowe, A. B.; Sumerlin, B. S.; McCormick, C. L. *Macromolecules* **2002**, *35*, 4123.
- Donovan, M. S.; Sanford, T. A.; Lowe, A. B.; Sumerlin, B. S.; Mitsukami, Y.; McCormick, C. L. *Macromolecules* **2002**, *35*, 4570.
- Millard, P.-E.; Barner, L.; Stenzel, M. H.; Davis, T. P.; Barner-Kowollik, C.; Müller, A. H. E. *Macromol. Rapid Commun.* **2006**, *27*, 821.
- Favier, A.; Charreyre, M.-T.; Chaumont, P.; Pichot, C. *Macromolecules* **2002**, *35*, 8271.
- Donovan, M. S.; Sumerlin, B. S.; Lowe, A. B.; McCormick, C. L. *Macromolecules* **2002**, *35*, 8663.
- D'Agosto, F.; Hughes, R.; Charreyre, M.-T.; Pichot, C.; Gilbert, R. G. *Macromolecules* **2003**, *36*, 621.
- De Lambert, B.; Charreyre, M.-T.; Chaix, C.; Pichot, C. *Polymer* **2007**, *48*, 437.
- Chong, B. Y. K.; Krstina, J.; Le, T. P. T.; Moad, G.; Potsma, A.; Rizzardo, E.; Thang, S. H. *Macromolecules* **2003**, *36*, 2256.
- Taton, D.; Wilckowska, A.; Z.; Destarac, M. *Macromol. Rapid Commun.* **2001**, *22*, 1497.
- Ladavière, C.; Dorr, N.; Clavierie, J. P. *Macromolecules* **2001**, *34*, 5370.
- Mayadunne, R. T. A.; Rizzardo, E.; Chiefari, J.; Chong, Y. K.; Moad, G.; Thang, S. H. *Macromolecules* **1999**, *32*, 6977.
- Destarac, M.; Charnot, D.; Franck, X.; Zard, S. Z. *Macromol. Rapid Commun.* **2000**, *21*, 1035.
- Schilli, C.; Müller, A. H. E.; Rizzardo, E.; Thang, S. H.; Chong, Y. K. In *Advances in Controlled/Living Radical Polymerization*; Matyjaszewski, K., Ed.; American Chemical Society: Washington, DC, 2003; Vol. 854.
- Schilli, C.; Lanzendörfe, M. G.; Müller, A. H. E. *Macromolecules* **2002**, *35*, 6819.
- Mayadunne, R. T. A.; Rizzardo, E.; Chiefari, J.; Krstina, J.; Moad, G.; Postma, A.; Thang, S. H. *Macromolecules* **2000**, *33*, 243.
- Convertine, A. J.; Ayres, N.; Scales, C. W.; Lowe, A. B.; McCormick, C. L. *Biomacromolecules* **2004**, *5*, 1177.

- (25) Lai, J. T.; Filla, D.; Shea, R. *Macromolecules* **2002**, *35*, 6754.
- (26) Pai, T. S. C.; Barner-Kowollik, C.; Davis, T. P.; Stenzel, M. H. *Polymer* **2004**, *45*, 4383.
- (27) Duwez, A.-S.; Guillet, P.; Colard, C.; Gohy, J.-F.; Fustin, C.-A. *Macromolecules* **2006**, *39*, 2729.
- (28) Moad, G.; Rizzardo, E.; Thang, S. H. *Aust. J. Chem.* **2005**, *58*, 349.
- (29) Perrier, S.; Takolpuckdee, P. *J. Polym. Sci., Part A: Polym. Chem.* **2005**, *43*, 5347.
- (30) Favier, A.; Charreyre, M.-T. *Macromol. Rapid Commun.* **2006**, *27*, 653.
- (31) Charreyre, M. T.; Mandrand, B.; Martinho, J. M. G.; Relogio, P.; Farinha, J. P. S. WO 07/003781, 2007.
- (32) Chen, M.; Ghiggino, K. P.; Mau, A. W. H.; Rizzardo, E.; Thang, S. H.; Wilson, G. J. *Chem. Commun.* **2002**, 2276.
- (33) Chen, M.; Ghiggino, K. P.; Launikonis, A.; Mau, A. W. H.; Rizzardo, E.; Sasse, W. H. F.; Thang, S. H.; Wilson, G. J. *J. Mater. Chem.* **2003**, *13*, 2696.
- (34) Chen, M.; Ghiggino, K. P.; Mau, A. W. H.; Rizzardo, E.; Sasse, W. H. F.; Thang, S. H.; Wilson, G. J. *Macromolecules*, **2004**, *37*, 5479.
- (35) Chen, M.; Ghiggino, K. P.; Mau, A. W. H.; Sasse, W. H. F.; Thang, S. H.; Wilson, G. J. *Macromolecules* **2005**, *38*, 3475.
- (36) Zhou, N.; Lu, L.; Zhu, X.; Yang, X.; Wang, X.; Zhu, J.; Zhou, D. *Polym. Bull. (Berlin)* **2006**, *57*, 491.
- (37) Chiefari, J.; Mayadunne, R. T. A.; Moad, C. L.; Moad, G.; Rizzardo, E.; Potsma, A.; Skidmore, M. A.; Thang, S. H. *Macromolecules* **2003**, *36*, 2273.
- (38) Ghosh, H. N. *J. Phys. Chem. B* **1999**, *103*, 10382.
- (39) Barik, A.; Kumbhakar, M.; Nath, S.; Pal, H. *Chem. Phys.* **2005**, *315*, 277.
- (40) (a) Lowe, A. B.; Sumerlin, B. S.; Donovan, M. S.; McCormick, C. L. *J. Am. Chem. Soc.* **2002**, *124*, 11562. (b) Sumerlin, B. S.; Lowe, A. B.; Stroud, P. A.; Zhang, P.; Urban, M. W.; McCormick, C. L. *Langmuir* **2003**, *19*, 5559.
- (41) Favier, A.; Ladavière, C.; Charreyre, M.-T.; Pichot, C. *Macromolecules* **2004**, *37*, 2026.
- (42) Favier, A.; Charreyre, M. T. WO 04/055060, 2004.
- (43) D'Agosto, F.; Charreyre, M. T.; Pichot, C. *Macromol. Biosci.* **2001**, *1*, 322.
- (44) D'Agosto, F.; Charreyre, M. T.; Veron, L.; Llauro, M. F.; Pichot, C. *Macromol. Chem. Phys.* **2001**, *202*, 1689.
- (45) de Lambert, B.; Charreyre, M. T.; Chaix, C.; Pichot, C. *Polymer* **2005**, *46*, 623.
- (46) Martinho, J. M. G.; Egan, L. S.; Winnik, M. A. *Anal. Chem.* **1987**, *59*, 861.
- (47) Farinha, J. P. S.; Martinho, J. M. G.; Pogliani, L. *J. Math. Chem.* **1997**, *21*(2), 131.
- (48) Marquardt, D. W. *J. Soc. Ind. Appl. Math.* **1963**, *11*, 431.
- (49) Lakowicz, J.R. In *Principles of Fluorescence Spectroscopy*; Plenum: New York, 1999.
- (50) Martinho, J. M. G. *J. Phys. Chem.* **1989**, *93*, 6687.
- (51) Farinha, J. P. S.; Martinho, J. M. G.; Xu, H.; Winnik, M. A.; Quirk, R. P. *J. Polym. Sci., Polym. Phys.* **1994**, *32*, 1635.
- (52) Qiu, X.-P.; Winnik, F. M. *Macromol. Rapid Commun.* **2006**, *27*, 1648.
- (53) Nakayama, M.; Okano, T. *Biomacromolecules* **2005**, *6*, 2320.

MA070444G